Multiquantum Vibrational Deactivation of $N_2^+(v)$ by Collisions with N_2 and O_2 at Thermal Energies

Shuji Kato, Veronica M. Bierbaum, and Stephen R. Leone*,†

JILA, National Institute of Standards and Technology and University of Colorado, Department of Chemistry and Biochemistry, University of Colorado, Boulder, Colorado 80309-0440

Received: March 30, 1998; In Final Form: June 3, 1998

Vibrational deactivation and charge transfer in the collisions of $N_2^+(v = 0-4)$ with N_2 and O_2 are studied at thermal energies. State-specific rate constants for the individual components of charge transfer and vibrational deactivation are determined using the selected-ion flow tube, laser-induced fluorescence technique. The $^{15}N_2^+(v = 0) + {}^{14}N_2$ reaction proceeds via symmetric charge transfer at one-half the Langevin rate constant ($0.5k_L$), indicating efficient charge equilibration, whereas the total removal rates of $v = 1-4$ ($\sim 6 \times 10^{-10}$ cm^3 molecule^{-1} s^{-1}) exceed $0.5k_L$. This indicates that vibrational transfer, in addition to charge equilibration, contributes to the removal of $N_2^+(v > 0)$ by collisions with N_2. The $N_2^+(v) + O_2$ removal rates are significantly enhanced upon vibrational excitation; the total rate constant for $v = 4$ is 3.0×10^{-10} cm^3 molecule^{-1} s^{-1}, six times larger than that for $v = 0$. The enhancement is shown to be primarily due to increased vibrational deactivation, although a small enhancement of the charge-transfer channel also occurs for $N_2^+(v \geq 2) + O_2$. Multiquantum vibrational energy transfer during single collisions plays an important role in the deactivation of $N_2^+(v \geq 2)$ with both N_2 and O_2. The occurrence of multiquantum deactivation is rationalized by the existence of significantly deep potential wells for $N_2^+-N_2$ and $N_2^+-O_2$, which arise from electron-exchange interactions. Small modifications are also made to the earlier studies on the reactions of $N_2^+(v \leq 2) + N_2$ (Frost, M. J.; et al. *J. Chem. Phys.* **1994**, *100*, 6359) and $N_2^+(v \leq 2) + O_2$ (Kato, S.; et al. *Can. J. Chem.* **1994**, *72*, 625).

Introduction

The effect of reactant internal-state excitation on ion−molecule reactions is of fundamental interest in state-selective and state-to-state chemistry.[1,2] A recent review details the effects of ion vibrational excitation, along with rotational excitation and neutral vibrational excitation, in a variety of ion−molecule reactions.[3] Vibrational excitation of ions can significantly alter the kinetics and dynamics of their reactions. For example, a dramatic enhancement was recently observed for the charge-transfer probability of the $N_2^+(v) + Kr$ reaction upon vibrational excitation,[4] a system where the reactions of all vibrational states are exothermic. When vibrationally excited ions collide with neutral molecules at thermal energy, deexcitation of vibration is another important channel that determines the outcome of the reaction. For the reactions of $N_2^+(v)$ with M (= N_2, O_2), charge transfer (eq 1) and vibrational deactivation (eq 2) are competing processes.

$$N_2^+(v = i) + M \rightarrow N_2 + M^+ \quad (1)$$

$$\rightarrow N_2^+(v < i) + M \quad (2)$$

The kinetics and dynamics of these vibrationally excited ion processes are important in the chemistry of the earth's ionosphere.[5,6] In addition, recent interest in plasma processes related to hypersonic flight provides compelling reasons for understanding the subject of ion deactivation and reactions in the atmosphere.[7]

Ferguson reviewed diatomic ion vibrational deactivation and proposed a mechanism of ion−molecule complex predissociation to successfully explain the magnitude of the deactivation rate constants.[8,9] However, little is known about the *dynamics* of ion vibrational deactivation for multiply excited vibrational states, e.g., how many vibrational quanta are lost per collision and how the energy is distributed. For neutral−neutral systems there are numerous experimental and theoretical studies on vibrational excitation/deactivation dynamics; the dominance of single quantum transitions ($|\Delta v| = 1$) at thermal energy is rationalized by the Landau−Teller theory for vibration-to-translation (V−T) energy transfer.[10,11] Similar models explain resonant vibration-to-vibration (V−V) energy transfer, primarily $\Delta v = \pm 1$, with great success.[10] The shortage of knowledge for ion−molecule deactivation dynamics is primarily due to experimental difficulties. A rare example of investigating the mechanism for vibrational deactivation of higher vibrational states in an ion−molecule system is the Fourier transform ion cyclotron resonance (FT-ICR) study of Wyttenbach and Bowers,[12] in which they report that the $\Delta v = -1$ transitions are the primary deactivation paths for $NO^+(v = 2,3)$ ions colliding with several neutral species.

More recently we used a selected-ion flow tube, laser-induced fluorescence (SIFT-LIF) instrument[13] to study the state-specific dynamics of $N_2^+(v)$ ions for relatively low vibrational excitation, $v = 0$, 1, 2. We observed simultaneous transfer of charge and

* To whom correspondence should be addressed. E-mail: SRL@JILA.Colorado.Edu. Facsimile: (303) 492-5504.

† Staff member, Quantum Physics Division, National Institute of Standards and Technology.

S1089-5639(98)01679-X CCC: $15.00
Published on Web 07/29/1998

vibration in the reaction of $^{15}N_2^+(v = 2) + {}^{14}N_2$ producing $^{14}N_2^+(v = 2)$ (with $^{15}N_2(v = 0)$ as the concomitant neutral product).[14,15] This is clear evidence of multiquantum V−V energy transfer and a violation of a simple $\Delta v = \pm 1$ idea at thermal energies. For reference, at higher collision energies ($E_{c.m.} > 1$ eV), there have been several studies of multiquantum T → V excitation for the $N_2^+ + N_2$ system.[16−20] Another violation of the $\Delta v = -1$ rule was observed for the $N_2^+(v = 2) + O_2$ reaction, for which the vibrational deactivation (eq 2) is significantly more efficient than charge transfer (eq 1) and $v = 2 \rightarrow v = 1$ and $v = 2 \rightarrow v = 0$ processes were both shown to occur.[21] The nature of multiquantum vibrational transfer in these systems is not fully understood with the limited experimental data. In addition, our study suggested a small but non-negligible enhancement of charge transfer for the $N_2^+(v = 2) + O_2$ reaction[21] while previous work reported that the charge-transfer rate is insensitive to vibrational excitation in this system.[22−24] The effect of vibration on the charge-transfer rate constant for $N_2^+(v) + O_2$ is yet to be completely resolved.

Our recent success[4] in detecting N_2^+ vibrational states up to $v = 4$ permits these questions to be addressed in further detail. Exploring higher vibrational states will give deeper insights into the transfer of charge and multiquantum vibrational deactivation in the $N_2^+(v) + N_2$ and O_2 reactions. In the present work, we determine the thermal-energy rate constants for charge transfer and vibrational deactivation for these reactions over a wider range of vibrational excitation ($v = 0-4$). By combining the results with previous data at lower vibrational excitation,[14,15,21] we characterize the vibrational energy dissipation in multiquantum transitions. This also brings about some modifications to the previous values and interpretations. We discuss the observed multiquantum vibrational deactivation in the $N_2^+(v) + N_2$, O_2 reactions in conjunction with the depth of the ion−molecule potential wells for these systems.

Experimental Section

The experiments were performed using the SIFT-LIF apparatus,[13] which consists of a selected ion flow tube (SIFT) and laser-induced fluorescence (LIF) detection. Briefly, vibrationally excited N_2^+ ions are produced by electron impact on ≈2.7 Pa (20 mTorr) of N_2. The N_2^+ ions are extracted, mass selected, and injected into the flow tube, where they are entrained in He carrier gas at a pressure of 80 Pa (0.6 Torr). The helium is supplied through two concentric annular inlets around the injection orifice. The injection potential of N_2^+ ions is 47 eV (lab-frame energy). The ions can acquire further vibrational excitation in the injection process, while they are rotationally and translationally thermalized by collisions with He.

For LIF detection of $N_2^+(X, v)$ in a specific vibrational level, a corresponding $B^2\Sigma_u^+ \leftarrow X^2\Sigma_g^+$ vibronic transition is excited by radiation from an excimer-pumped dye laser operated at a typical repetition rate of 100 Hz. The LIF detection point is located ≈11 cm downstream of the injection orifice. An improvement in ion injection efficiency and LIF detection sensitivity[4] enables us to detect $N_2^+(v)$ ions in higher vibrational states than previously studied in the O_2 and N_2 reactions; N_2^+ vibrational levels populated up to $v = 4$ are investigated. The vibrational population distribution of $N_2^+(v)$, determined previously with LIF, is 0.46 ($v = 0$), 0.23 ($v = 1$), 0.15 ($v = 2$), 0.12 ($v = 3$), 0.04 ($v = 4$), and <0.01 ($v = 5$, not observed), at an injection potential of 47 eV.[4] The proximity of the laser detection to the injection orifice facilitates LIF detection of $N_2^+(v)$ with good signal-to-noise (typically 2−10 photons s^{-1} at the band head positions).

Nitrogen (>99.998%) or oxygen (>99.998%) is added through a reactant inlet placed between the injection orifice and the LIF detection point, at a distance of 4.4 cm from the orifice. The inlet has 18 pinholes equally spaced around the inner wall of the flow tube in order to provide uniform mixing of the reactant gas with He. The reactant flow meter has been calibrated over the flow range studied. Laser-induced fluorescence is used to monitor the change in $N_2^+(v)$ density due to the reaction with the added N_2 or O_2. The dye laser is tuned to a specific band head position of $N_2^+(v)$ and signals are collected for a given flow rate of reactant. A full kinetic decay is obtained by changing the flow rate and observing the change in signal intensity, providing information on the state-specific removal of $N_2^+(v)$ with N_2 and O_2. Since the He flow is turbulent rather than laminar in the reaction region when relatively close to the venturi inlet, direct absolute determination of rate constants by this method would be difficult. Instead we use the $N_2^+(v = 1) + Ar$ charge transfer as a reference reaction, for which the absolute rate constant is known to be 4×10^{-10} cm^3 $molecule^{-1}$ s^{-1}.[25] This system has proven to be an excellent reaction for calibrating other reaction rate constants.[26,27]

Kinetic Modeling and Analysis

Principles of Analysis. Experimental kinetic plots for $N_2^+(v = i) + N_2$ and $N_2^+(v = i) + O_2$ are analyzed using the following models to extract vibrationally state-specific rate constants, $k_{CT,i}$ (charge transfer, eq 1) and $k_{q,i}$ (vibrational deactivation, eq 2). The rate constant $k_{q,i}$ is given as the sum of state-to-state deactivation rate constants for transitions $v = i \rightarrow v = i - 1, i - 2, ...,$ and 0. Although multiple collisions occur in these flow tube experiments, the extracted rate constants provide information on the state-specific and state-to-state processes. The rotational distributions remain thermalized by collisions with the He buffer gas, but the vibrational data are extrapolated to obtain state-resolved limits. The key issue of the present study is to examine whether multiquantum vibrational deactivation ($|\Delta v| > 1$) occurs for collisions of $N_2^+(v \geq 2)$ with N_2 or O_2.

The vibrational deactivation components are considered first. Relevant vibrational constants are N_2^+ ($\omega_e = 2207.37$ cm^{-1}), N_2 ($\omega_e = 2358.57$ cm^{-1}), and O_2 ($\omega_e = 1580.39$ cm^{-1}).[28] Vibrational deactivation of $N_2^+(v)$ with N_2 is expected to be primarily via V−V processes because of the near resonance of the vibrational energy and the available collision energy in the experiment (<0.1 eV).[13] Although ion vibrational deactivation does not always follow resonance principles,[27] the existence of efficient V−V energy transfer is obvious for the $N_2^+(v) - N_2$ system.[14,15] In collisions with O_2, on the other hand, $N_2^+(v)$ ions can also be expected to be deactivated via vibration-to-rotation, translation (V−R,T) processes. Figure 1 schematically shows the assumed models for $N_2^+(v)$ vibrational relaxation for the case of $v = 4$. Upon a single collision with the neutral reactant, $N_2^+(v = 4)$ can relax exclusively to $v = 3$ ($\Delta v = -1$ transfer; model 1), relax equally to $v = 3, 2, 1, 0$ (model 3), or relax exclusively to $v = 0$ (model 4). The energy removed from $N_2^+(v = 4)$ is transferred to the vibration of the neutral reactant (V−V) or dissipated into other degrees of freedom of the departing fragments (V−R,T). These three models are examined, along with model 2, which is an intermediate case between models 1 and 3.

Second, the magnitudes of the charge-transfer components may depend on the vibrational excitation of N_2^+. For charge transfer of $N_2^+(v \geq 2)$ with O_2, the electronically excited $O_2^+(a^4\Pi_u)$ product state becomes energetically accessible (eq

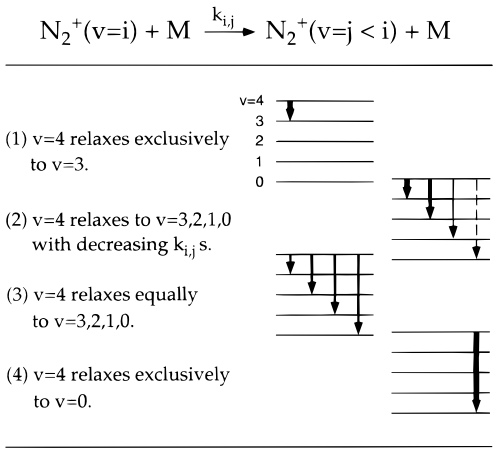

Figure 1. Models for $N_2^+(v)$ vibrational relaxation upon a single collision with reactant M. Relaxation of $v = 4$ is schematically shown; the thickness of the arrows represents the relative magnitudes of $k_{i,j}$.

3) and the charge transfer may be expected to be enhanced for $v \geq 2$.

$$N_2^+(v = 2) + O_2 \rightarrow N_2 + O_2^+(a^4\Pi_u) + 0.012 \text{ eV} \quad (3)$$

In fact, an enhancement of ≈50% was suggested in our recent mass spectrometric measurement.[21] For near-resonant $N_2^+(v)$ + N_2 collisions, the charge is expected to be completely randomized between the two nitrogen species, as indicated by the $^{15}N_2^+(v = 0) + {}^{14}N_2$ reaction, which proceeds nearly exactly at one-half the Langevin collision rate ($0.51k_L$).[15]

The principles of the analysis are to assume a set of vibrationally dependent charge-transfer rate constants and then search for the best model for vibrational deactivation. This procedure is continued until the combination of charge transfer and vibrational deactivation models is found that best describes the experimental results. Rate constants for charge transfer and vibrational deactivation are then extracted, accordingly. It is noted that the models are analytical and can only describe the overall *outcome* of the experiments. Actual collisional events may involve dynamical competitions between charge transfer and vibrational deactivation. For example, two successive charge-transfer events during a single collision could result in vibrational deactivation without a net charge transfer. Nevertheless, the models are designed to describe the outcome of the experimental observables in the present study. Specific considerations for the analyses of $N_2^+(v)$ + O_2 and $N_2^+(v)$ + N_2 systems are given below.

$N_2^+(v)$ + O_2 Analysis. Charge transfer of $N_2^+(v)$ to O_2 depopulates the level $v = i$ with a state-specific charge-transfer (CT) rate constant $k_{CT,i}$. In the present modeling of charge transfer, we include various degrees of vibrational enhancement of $k_{CT,i}$ (0−100%), on average for $v \geq 2$ with respect to $v = 0$ and $v = 1$. The CT rate constant for $v = 0$ is taken to be the same as obtained previously ($k_{CT,0} = 0.49 \times 10^{-10}$ cm^3 molecule^{-1} s^{-1}).[21] This value approximately represents an average of a number of previous values (summarized in ref 21) and also is found to fit the $v = 0$ plot reasonably well in the present refined analysis. Under the thermal energy conditions in the present study, the vibrational deactivation takes place from $v = i$ to $v = j$ ($j < i$) with rate constants $k_{i,j}$ as modeled in Figure 1.

For each model, we solve coupled differential equations for $N_2^+(v)$ + O_2 and fit experimental kinetic plots. Briefly, when a total rate of loss for the ith level, k_i ($= k_{CT,i} + k_{q,i}$), is known, the sum of probabilities for the vibrational deactivation to lower levels is given by

$$\sum_{j<i} k_{i,j} \equiv k_{q,i} = k_i - k_{CT,i} \quad (4)$$

Each $k_{i,j}$ is derived using one of the assumed forms for vibrational deactivation (Figure 1). The deactivation probabilities from higher-lying hth levels ($h > i$) are used to describe the kinetics of the ith level

$$\frac{d[N_2^+(v = i)]}{[M]dt} = \sum_{h>i} k_{h,i}[N_2^+(v = h)] - k_i[N_2^+(v = i)] \quad (5)$$

where [M] is the concentration of the neutral reactant (M = O_2 for eq 5). Equation 5 is used to fit the kinetic plot of the ith level to derive k_i, which then is used to determine the vibrational deactivation from the ith level using eq 4. The total rate of loss for $v = 4$ (k_4) is readily determined since the contribution from higher levels is negligible.

$N_2^+(v)$ + N_2 Analysis. The $N_2^+(v)$ + N_2 reaction is a symmetric CT system, and the kinetic analysis is more complicated, because the charge-transfer reaction regenerates N_2^+ products that can further react with N_2 neutral. A single collision of $^{15}N_2^+(v = i)$ with $^{14}N_2(v = 0)$ at thermal energy produces reaction products according to

$$^{15}N_2^+(v = i) + {}^{14}N_2(v = 0) \xrightarrow{k^*_{i,j}} {}^{15}N_2^+(v = j) + {}^{14}N_2(v = n) \quad (6)$$

$$\xrightarrow{k^{CT}_{i,j}} {}^{15}N_2(v = n) + {}^{14}N_2^+(v = j) \quad (7)$$

where j and n denote the vibrational quantum numbers for ionic and neutral products, respectively, and the asterisk denotes the rate constants for $^{15}N_2^+$ species. Equation 6 represents pure vibrational deactivation within the $^{15}N_2^+$ manifold ($j < i$), whereas eq 7 describes pure CT without a change in vibration ($n = i$ and $j = 0$) or simultaneous change in the vibrational and charge states ($j > 0$). Conditions $j + n = i$ and $j + n < i$ correspond to V−V and V−R,T transfers, respectively. The ionic products from eqs 6 and 7 ($^{15}N_2^+$ and $^{14}N_2^+$, respectively) can further react with $^{14}N_2$. For the subsequent reaction of $^{14}N_2^+(v)$ with $^{14}N_2$

$$N_2^+(v = i) + N_2(v = 0) \xrightarrow{k_{i,j}} N_2^+(v = j) + N_2(v = n) \quad (8)$$

where

$$k_{i,j} = k^*_{i,j} + k^{CT}_{i,j} \quad (9)$$

For the $^{14}N_2^+(v)$ + $^{14}N_2$ reaction, the experimentally observed quantity ($k_{i,j}$) is actually the sum of the components for pure vibrational transition and that accompanying charge transfer (eq 9). An assumption in the use of $k^*_{i,j}$ and $k^{CT}_{i,j}$ in eqs 6, 7, and 9 is that there are negligible isotope effects for the vibrational relaxation and charge-transfer probabilities between $^{15}N_2^+(v)$ + $^{14}N_2$ and $^{14}N_2^+(v)$ + $^{14}N_2$. This is reasonable in view of the similar energetics and Franck−Condon overlaps. For simplicity, the above reactions are designated as $(i^+,0) \rightarrow (j^+,n)$ for eqs 6 and 8 and $(i^+,0) \rightarrow (n,j^+)$ for eq 7.

The $^{15,14}N_2^+(v) + N_2$ reactions are modeled as follows. First, charge is assumed to be completely randomized between the two nitrogen species by the collision, as experimentally proven for the $^{15}N_2^+(v = 0) + {}^{14}N_2$ reaction.[15] The charge exchange can take place both within the intimate $N_2^+-N_2$ collision complex and at a longer range, but within the Langevin diameter. Second, energy dissipation for V−V and V−R,T transfers are modeled as in Figure 1. The V−V and V−R,T processes can take place within the intimate complex, while the V−V transfer may also take place at a long range by virtue of the charge-induced dipole interactions,[1] despite the absence of permanent dipoles or dipole derivatives for N_2^+ and N_2. Energetically, many of the V−V and charge-transfer processes are slightly endothermic, but the energy gaps are within the collision energies in the SIFT-LIF instrument (<0.1 eV)[13] and hence these processes are accessible. In any event, the efficient charge randomization overrides the vibrational transfer so that product pairs with the same vibrational partition but with different charge location, e.g., $(3^+,1)$ and $(3,1^+)$, will have the same probabilities of formation.

For the $^{15}N_2^+(v) + {}^{14}N_2$ reaction, the concentration of the $^{15}N_2^+(v = i)$ reactant is described by

$$\frac{d[^{15}N_2^+(v=i)]}{[M]dt} = \sum_{h>i} k^*_{h,i}[^{15}N_2^+(v=h)] - k^*_i[^{15}N_2^+(v=i)] \quad (10)$$

where

$$k^*_i = \sum_{j<i} k^*_{i,j} + \sum_{j\le i} k^{CT}_{i,j} \quad (11)$$

The evolution of the $^{14}N_2^+(v = i)$ product is described by

$$\frac{d[^{14}N_2^+(v=i)]}{[M]dt} = \sum_{h>i} k_{h,i}[^{14}N_2^+(v=h)] + \sum_{h\ge i} k^{CT}_{h,i}[^{15}N_2^+(v=h)] - k_i[^{14}N_2^+(v=i)] \quad (12)$$

where

$$k_i = \sum_{j<i} k_{i,j} = \sum_{j<i} (k^*_{i,j} + k^{CT}_{i,j}) \quad (13)$$

Note that a term $k^{CT}_{i,i}$ in eq 11 is missing in eq 13, since it is indistinguishable. For the $^{14}N_2^+(v) + {}^{14}N_2$ reaction, the second term in eq 12 disappears and the observed kinetic loss of $^{14}N_2^+(v = i)$ is described by

$$\frac{d[^{14}N_2^+(v=i)]}{[M]dt} = \sum_{h>i} k_{h,i}[^{14}N_2^+(v=h)] - k_i[^{14}N_2^+(v=i)] \quad (14)$$

where k_i is given by eq 13.

The total rate of loss for the ith level (k^*_i for $^{15}N_2^+$ or k_i for $^{14}N_2^+$) is determined by fitting the kinetic plot for $v = i$ with eq 10 or eq 14. Dynamic plots for the appearance and decay of the $^{14}N_2^+(v = 1$ or $2)$ product in the $^{15}N_2^+(v) + {}^{14}N_2$ system are analyzed by using eq 12. In practical analyses of $N_2^+(v) + N_2$ collisions, Figure 1 should also include $\Delta v = 0$, CT processes, i.e., $(m^+,0) \rightarrow (m,0^+)$ transitions, which may be efficient because of the dominantly large Franck−Condon factors (0.84, 0.70, 0.56, 0.43, and 0.32 for $m = 0$, 1, 2, 3, 4, respectively). The experimental plots are best fit by a proper combination of the above CT and V−V/V−R,T models, which further incorporates contributions of the $\Delta v = 0$, CT processes.

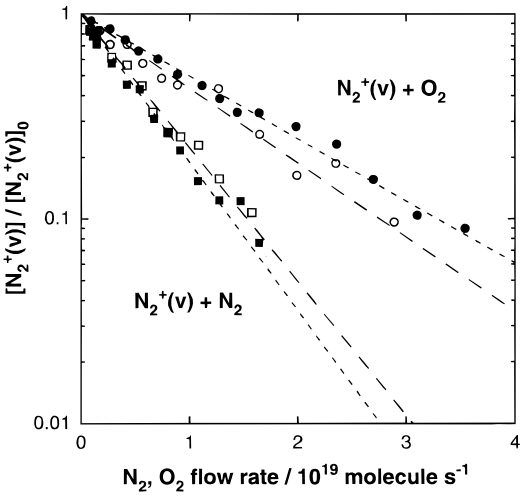

Figure 2. LIF kinetic plots for $N_2^+(v = 3, 4)$ with N_2 and O_2. The LIF signal intensity for $N_2^+(v)$ is normalized to that at zero reactant flow ($\equiv [N_2^+(v)]_0$). $N_2^+(v = 3) + N_2$ (■), $N_2^+(v = 4) + N_2$ (□), $N_2^+(v = 3) + O_2$ (●), and $N_2^+(v = 4) + O_2$ (○). The associated lines are the single-exponential fits to the data.

Results

Raw Rate of Loss. Kinetic plots for the $^{14}N_2^+(v = 3, 4) + O_2$ and N_2 reactions are shown in Figure 2. The raw plots reflect the evolution of $N_2^+(v)$ due to charge transfer and vibrational deactivation. If vibrational cascading occurs significantly from these higher levels, it accumulates into the lower vibrational levels and their kinetics can be considerably affected. The purpose of this section is first to gain a sense for the magnitudes of the "raw" rates of total loss and to set guidelines for the exact analyses to extract the "real" rates of total loss and the components for charge transfer and vibrational deactivation.

Upon collisions with O_2 or N_2, the $N_2^+(v = 3, 4)$ signals decay faster than do the $N_2^+(v \le 2)$ signals reported earlier.[15,21] The raw rates of loss for $v = 3$ and $v = 4$ are obtained by simply fitting single exponentials to the LIF kinetic plots (Figure 2). These rate constants, along with the raw rate constants for $v \le 2$ from previous measurements,[15,21] are shown in Figure 3. The error bars for these rate constants ($\pm 1\sigma$) are typically within the size of the symbols. The rate constant for $N_2^+(v = 0) + N_2$ was separately determined from the isotopically labeled $^{15}N_2^+(v = 0) + {}^{14}N_2$ reaction.[15] Although the decay profiles for $N_2^+(v = 0,1)$ with O_2 obviously deviate from single exponentials (Figure 5 in ref 21), the apparent raw rate constants are shown in Figure 3 nevertheless.

The raw rates of loss for the $N_2^+(v) + O_2$ reactions are dramatically enhanced by vibrational excitation of the reactant ion. The rate for the uppermost level $v = 4$ is 3.0×10^{-10} cm^3 molecule^{-1} s^{-1}, amounting to ≈40% of the Langevin collision rate (7.67×10^{-10}) and about six times greater than that for $v = 0$ (0.49×10^{-10}). The kinetics of $N_2^+(v = 4)$ is little affected by $N_2^+(v > 4)$, because the $v > 4$ concentration is negligible, and hence the raw rate for $v = 4$ essentially represents the real rate of total loss. Since the charge transfer of $N_2^+(v = 0)$ with O_2 is slow and the CT is enhanced by no more than a factor of 2 on average for $v = 2-4$ (mass spectrometric experiment in ref 21), the enhanced reactivity for $v = 1-4$ arises primarily

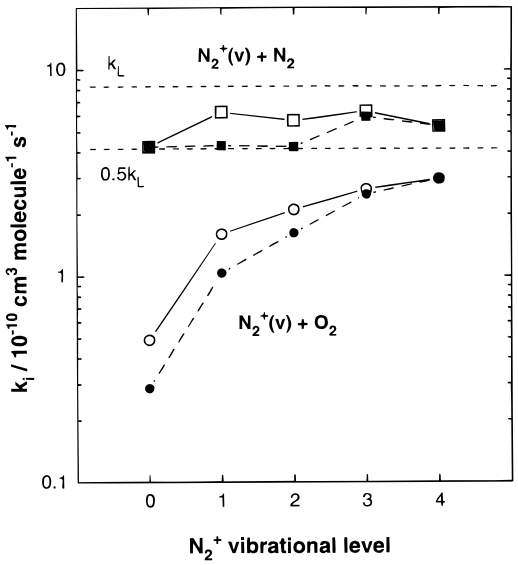

Figure 3. Total rates of removal for $N_2^+(v) + N_2$ (squares) and O_2 (circles) as a function of the N_2^+ vibrational excitation. Single-exponential fits to the LIF kinetic plots give "raw" rates (closed symbols). The "real" rates for total loss, after correction for vibrational relaxation, obtained from the best fits (see text), are shown by the open symbols. Horizontal lines indicate the Langevin ($k_L = 8.3 \times 10^{-10}$ cm^3 molecule^{-1} s^{-1}) and one-half the Langevin collision rate constants for $N_2^+ + N_2$.

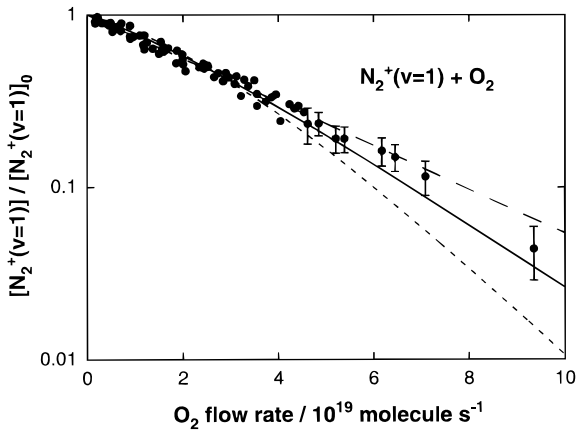

Figure 4. LIF kinetic plot for $N_2^+(v = 1) + O_2$. Data reported earlier in ref 21. The LIF signal intensity for $N_2^+(v = 1)$ is normalized to that at zero O_2 flow ($\equiv [N_2^+(v = 1)]_0$). Also shown are simulations assuming that vibrational relaxation occurs via $\Delta v = -1$ transfer (short dashed line; no enhancement in the CT rates), equal transfer to lower levels (solid line, 50% enhancement in the $v \geq 2$ CT rates), and exclusive transfer to $v = 0$ (long-dashed line, 0−100% enhancement in the $v \geq 2$ CT rates).

from vibrational deactivation. Exact rate constants for the deactivation and the amount of energy lost per collision will be discussed below.

The raw rates of loss for the $^{14}N_2^+(v = 3, 4) + N_2$ reactions are greater than half-Langevin ($\approx 0.7k_L$) where k_L is 8.30×10^{-10} cm^3 molecule^{-1} s^{-1}. This is in clear contrast to the previous observations for $v \leq 2$ where the raw rates are $\approx 0.5k_L$.[15] In general for symmetric charge-transfer systems, half-Langevin rate constants are expected when the (m^+,0) reactant state forms (m^+,0), (m,0$^+$) product states (no V−V transfer) and/or (0$^+$,m), (0,m^+) states (complete V−V transfer). The fact that the rate constants for $v = 3$ and 4 are greater than $0.5k_L$ indicates that in the $N_2^+(v = 3, 4) + N_2$ reactions other product states must also be formed via mechanisms of V−V transfer and possibly V−R,T transfer. It then follows that the analysis of the $v = 2$ and 1 kinetic plots should also take into account the contributions of vibrational deactivation from these upper levels. Consequently, the real rates of total loss for $N_2^+(v = 1$ and 2) will also be greater than $0.5k_L$. The kinetic plots for $^{14}N_2^+(v = 1-4)$, along with the kinetic and dynamic plots of $^{15}N_2^+(v = 1, 2) + N_2$, will be analyzed further below.

$N_2^+(v)$ + O_2 Reaction. All the models for vibrational deactivation (Figure 1) can reproduce the kinetic plots of the higher vibrational levels, $N_2^+(v = 2-4) + O_2$, equally well, regardless of the assumed enhancement of charge transfer for $v \geq 2$ (0−100%). However, for lower vibrational levels ($v \leq 1$), the simulations predict different kinetic plots depending on the model parameters assumed. Figure 4 shows the kinetic plot of $N_2^+(v = 1) + O_2$ and the results of several model fits. The fit profile assuming $\Delta v = -1$ processes (model 1 in Figure 1) deviates from the experimental plot beyond the error bars for higher O_2 flow rates. While pertaining to the $\Delta v = -1$ principle, agreement between the experiment and simulation is not appreciably improved by altering the degrees of CT enhancement (0−100%). In terms of the χ^2 values, better fits are obtained by assuming that higher vibrational levels relax

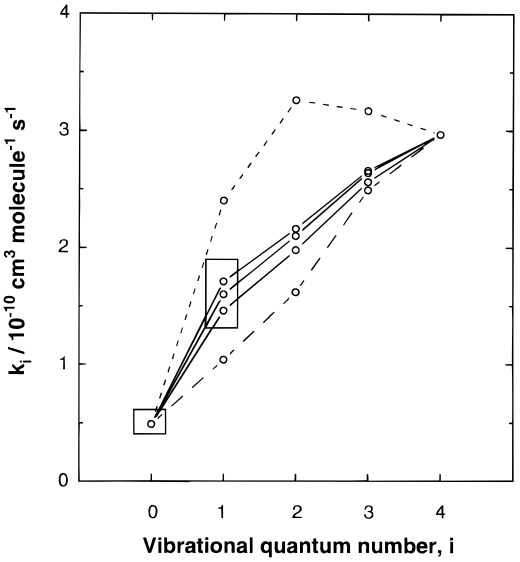

Figure 5. Total rates of removal for $N_2^+(v) + O_2$ as a function of the vibrational quantum number in N_2^+. The rate constants are derived by analyzing the LIF kinetic plots assuming that vibrational relaxation occurs via $\Delta v = -1$ (short-dashed line; no enhancement in the $v \geq 2$ CT rates), equal transfer to lower levels (solid lines), and exclusive transfer to $v = 0$ (long-dashed line; 0−100% enhancement in the $v \geq 2$ CT rates). The solid lines assume an enhancement in the $v \geq 2$ CT rates by 0% (top), 50% (middle), and 100% (bottom). The boxes indicate the ranges of the rate constants previously reported for $N_2^+(v = 0)$ and $N_2^+(v = 1)$.

equally to lower levels (model 3 in Figure 1) or relax exclusively to $v = 0$ (model 4 in Figure 1). The fits suggest the existence of multiquantum vibrational deactivation for $N_2^+(v \geq 2) + O_2$.

Although a single kinetic plot cannot uniquely determine the form of the vibrational relaxation, derived sets of rate constants ($v = 0-4$) are found to be quite sensitive to the model assumptions. Figure 5 presents the total rates of loss for $N_2^+(v = 0-4)$ with O_2, which are obtained from model fits assuming that the vibrational deactivation occurs via model 1 ($\Delta v = -1$ processes), model 3 (relaxing equally to lower levels), or model 4 (relaxing exclusively to $v = 0$). Fit results with

0%, 50%, and 100% CT enhancements are also shown for model 3 (solid lines). The fitting errors for $v \geq 1$ rate constants are within ± 0.07 ($\times 10^{-10}$ cm^3 molecule^{-1} s^{-1}) so that the fitting results are significant compared to each other. Figure 5 also indicates with boxes the ranges of rate constants previously reported for $v = 1$ ($1.3-1.9 \times 10^{-10}$ cm^3 molecule^{-1} s^{-1}, including possible error bars)[22-24] and for $v = 0$ ($0.4-0.6 \times 10^{-10}$ cm^3 molecule^{-1} s^{-1}).[21] The range of the rate constant for $v = 1$ can be used to distinguish the models assumed. Once again, the $\Delta v = -1$ model significantly overestimates the rate constant for $v = 1$ and hence is ruled out. Model 4, which assumed that all the vibration is relaxed exclusively to $v = 0$, now fails to predict the rate constant for $v = 1$. Good agreement is obtained when vibrational energy is assumed to relax equally to lower levels (model 3), regardless of the assumed degrees of CT enhancement (0−100%). Since model 3 predicts significantly larger rate constants for $v \geq 2$ than for $v = 1$, the vibrational excitation of $N_2^+(v > 0)$ in the previous studies[22-24] shown by the box is likely to be $v = 1$, as postulated in the present analysis.

The $N_2^+(v = 0) + O_2$ kinetic plot (Figure 5c in ref 21), which is most sensitive to the charge-transfer loss rate for $v > 0$, is similarly analyzed. For model 3 in which the vibrational energy relaxes equally to lower levels, the χ^2 values in fitting the kinetic plot for $v = 0$ are 0.180, 0.135, and 0.162 for the assumed CT enhancement of 0%, 50%, and 100%, respectively. The local minimum in the χ^2 values suggests that the charge-transfer rate is likely to be enhanced by $\approx 50\%$ on average for $v \geq 2$ (i.e., $k_{CT,i} \approx 0.75 \times 10^{-10}$ cm^3 molecule^{-1} s^{-1}), which is consistent with the previous estimate from the mass kinetics experiment.[21] If no enhancement is assumed for the $v \geq 2$ charge-transfer rates, the best fit to the $v = 0$ plot is obtained by increasing the value of $k_{CT,0}$ to 0.55×10^{-10} cm^3 molecule^{-1} s^{-1}. However, the χ^2 value is significantly larger (0.321), and this hypothesis of constant values for all $k_{CT,i}$ is not plausible.

In summary, the relaxation of $N_2^+(v \geq 2) + O_2$ includes a substantial contribution of multiquantum vibrational deactivation in a single collision. We also examined a model in which vibrational relaxation occurs to lower levels with decreasing $k_{i,j}$'s (model 2 in Figure 1), but this model is not found to be as satisfactory as model 3, which assumes equal relaxation to lower levels. The "real" rates of total loss for $N_2^+(v) + O_2$ (Figure 3) are taken from the best fits using model 3 (with 50% enhancement of charge transfer for $v \geq 2$), i.e., $3.0(\pm 0.2) \times 10^{-10}$, 2.6×10^{-10}, 2.1×10^{-10}, 1.6×10^{-10} and $0.49(\pm 0.02) \times 10^{-10}$ cm^3 molecule^{-1} s^{-1} for $v = 4$, $v = 3$, $v = 2$, $v = 1$, and $v = 0$, respectively. Error bars for the $v = 1$ to $v = 3$ rate constants are relatively difficult to estimate, but errors of $\pm 30\%$ account for the statistical errors, the model assumptions (models 2−4), and the range of the CT enhancement assumed (0−100%). With the refined analysis including $v = 3$ and $v = 4$, the total rate constants and vibrational deactivation rate constants for $v = 1$ and $v = 2$ become somewhat larger ($\sim 30\%$) than those previously reported.[21] However, the vibrational deactivation scheme for $N_2^+(v = 2) + O_2$ remains unchanged, i.e., both $v = 2 \rightarrow v = 1$ and $v = 2 \rightarrow v = 0$ processes are occurring.

$N_2^+(v) + N_2$ Reaction. In previous studies,[14,15] we found that $^{15}N_2^+(v = 2)$ is removed faster with $^{14}N_2$ than is $^{14}N_2^+(v = 2)$ because the symmetric CT channel is not observable for $^{14}N_2^+(v = 2)$. In addition, $^{14}N_2^+(v = 2)$ is produced by the $^{15}N_2^+(v = 2) + {}^{14}N_2$ reaction. We rationalized those results by the existence of simultaneous transfer of charge and two vibrational quanta, i.e., the $k^{CT}_{2,2}$ process in eq 11. The decay of $^{14}N_2^+(v = 2)$ can be slower because the $k^{CT}_{2,2}$ process merely regenerates the reactant ion. The production of $^{14}N_2^+(v = 2)$ from the $^{15}N_2^+(v = 2) + {}^{14}N_2$ reaction reflects directly the $k^{CT}_{2,2}$ process.

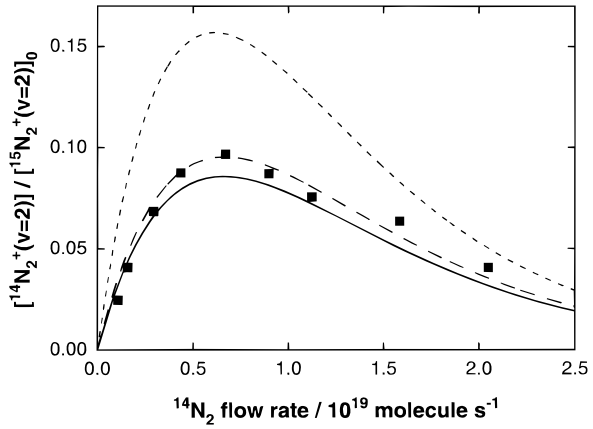

Figure 6. LIF dynamic plot for the appearance of $^{14}N_2^+(v = 2)$ signals from the reaction $^{15}N_2^+(v) + {}^{14}N_2 \rightarrow {}^{15}N_2 + {}^{14}N_2^+(v = 2)$. Data reported earlier in ref 14, with recalibration of the reactant flow rate. The LIF signal intensity for the $^{14}N_2^+(v = 2)$ product, $[^{14}N_2^+(v = 2)]$, is normalized to that for $^{15}N_2^+(v = 2)$ at zero $^{14}N_2$ flow, $[^{15}N_2^+(v = 2)]_0$. Also shown are simulations assuming that V−V relaxation occurs equally to lower levels (short-dashed line), V−V relaxation occurs equally to lower levels with an additional component ($0.2k_L$) of V−R,T relaxation (solid line), and V−V relaxation occurs exclusively to $v = 0$ with additional V−R,T relaxation (long-dashed line).

When higher vibrational states ($v = 3$ and 4) exist, however, the above observations may be rationalized differently. For example, if the charge and vibration are equipartitioned, the reaction of $^{15}N_2^+(v = 4)$ with $^{14}N_2$ can also produce $^{14}N_2^+(v = 2)$. The reaction of $^{14}N_2^+(v = 4) + {}^{14}N_2$ produces $^{14}N_2^+(v = 2)$ two times faster than $^{15}N_2^+(v = 4) + {}^{14}N_2$ produces $^{15}N_2^+(v = 2)$. Thus the kinetic decay of $^{14}N_2^+(v = 2)$ can also be slower than that of $^{15}N_2^+(v = 2)$, as observed.

Figure 6 shows the production of $^{14}N_2^+(v = 2)$ from the reaction of $^{15}N_2^+(v) + {}^{14}N_2$, where the $^{15}N_2^+(v)$ is a mixture of vibrational states up to $v = 4$. Obviously, the production of $^{14}N_2^+(v = 2)$ cannot be expected from V−R,T transfer, single-quantum V−V transfer, or combinations thereof. Multiquantum V−V processes must be occurring. However, the multiquantum V−V transfer alone cannot reproduce the experimental results. Among the models in Figure 1, we examine model 3 (vibrational relaxation occurring equally to lower levels) and model 4 (vibrational relaxation exclusively to $v = 0$). Model 2, in which vibration relaxes to lower levels with decreasing probabilities, is found to give less satisfactory results. With only the multiquantum V−V transfer, the simulation with model 3 significantly overestimates the observed appearance of $^{14}N_2^+(v = 2)$ (Figure 6). Model 4 is not consistent with the kinetic results (Figure 2) that $k_i > 0.5k_L$ for $^{14}N_2^+(v = 3,4) + N_2$. According to this model, for example, the product states from the $(4^+,0)$ reactant are $(4^+,0)$, $(4,0^+)$, $(0^+,4)$, and $(0,4^+)$ and thus $k_4 = 0.5k_L$ should result.

Thus the multiquantum V−V transfer of $N_2^+(v) + N_2$ must be accompanied by an additional component of V−R,T transfer. With the addition of V−R,T processes, models 3 and 4 are shown to reproduce the experimental results equally well (Figure 6). For simplicity, we assume that the V−R,T transfer proceeds via $\Delta v = -1$ transitions. For model 3, the best fit is obtained when the rate constant for the V−R,T process ($k_{V-R,T}$), i.e, the sum of the rates for production of $(m - 1^+,0)$ and $(m - 1,0^+)$ states from the reactant state $(m^+,0)$ is assumed to be $\approx 0.2k_L$.

TABLE 1: Product Distributions from a Single Collision of $^{15}N_2^+(v = 2) + {}^{14}N_2$

reactant state	product state[a]	reaction exothermicity/eV	product branching[b] model 3[c]	product branching[b] model 4[d]
$(2^+, 0)$	$(2^+, 0)$	0.000	0.21	0.16
	$(1^+, 1)$	−0.032	0.10	0
	$(0^+, 2)$	−0.057	0.10	0.16
	$(2, 0^+)$	−0.037	0.21	0.16
	$(1, 1^+)$	−0.031	0.10	0
	$(0, 2^+)$	−0.017	0.10	0.16
	$(1^+, 0)$	+0.257	0.09	0.18
	$(1, 0^+)$	+0.239	0.09	0.18

[a] For example, the $(0, 2^+)$ product state stands for $^{15}N_2(v = 0) + {}^{14}N_2^+(v = 2)$. [b] Expressed in units of k_L ($= 8.30 \times 10^{-10}$ cm^3 molecule^{-1} s^{-1}). Associated error bars are approximately ±10% of the values shown. [c] V−V relaxation occurs equally to $v = 1$ and $v = 0$. [d] V−V relaxation occurs exclusively to $v = 0$.

Even for model 3 in which $^{14}N_2^+(v = 2)$ can be populated by vibrational cascading from higher levels, the cascading accounts for only less than half of the $^{14}N_2^+(v = 2)$ appearance. Therefore the $k^{CT}_{2,2}$ transition is a real process. With model 4, the appearance of $^{14}N_2^+(v = 2)$ is due entirely to the $k^{CT}_{2,2}$ process.

Table 1 shows the best fit product distributions for a single collision of $^{15}N_2^+(v = 2) + {}^{14}N_2$, which are derived from the analyses using both models 3 and 4. The simultaneous transfer of charge and two vibrational quanta leading to the product state $(0, 2^+)$ is shown to take place with probabilities of 10% and 16% for models 3 and 4, respectively. Only these models can also reproduce the kinetic plots[14] for $^{14,15}N_2^+(v = 2) + {}^{14}N_2$ and kinetic[15] and dynamic[14,15] plots for $^{14,15}N_2^+(v = 1) + {}^{14}N_2$ fairly well. The "real" rates of total loss for $^{14}N_2^+(v) + N_2$ reactions are obtained from model 3 as 5.3×10^{-10} ($v = 4$), 6.3×10^{-10} ($v = 3$), 5.7×10^{-10} ($v = 2$), 6.2×10^{-10} ($v = 1$) and 4.2×10^{-10} cm^3 molecule^{-1} s^{-1} ($v = 0$), and are presented in Figure 3. Model 4 gives rate constants that are similar to those from model 3, with the exception of a value of 5.2×10^{-10} cm^3 molecule^{-1} s^{-1} for $v = 1$. The rate constants for $v = 2$ and $v = 1$ are now greater than $0.5k_L$ (4.15×10^{-10}), as opposed to the previous report.[15] In summary, although the experiment alone cannot determine which model is more likely, the analyses reveal a substantial amount of multiquantum V−V transfer occurring for the $N_2^+(v \geq 2) + N_2$ system.

We comment on a subtle issue related to the experiment and analysis for $N_2^+(v) + N_2$. Previous measurements[15] showed a negligible difference between the kinetic plots of $v = 1$ at different injection potentials (47 and 25 V), i.e., at different vibrational population distributions between $v = 2$ and $v = 1$. That observation appears to support model 4 rather than model 3; according to model 4 the $v = 1$ kinetics is insensitive to the vibrational population of $v > 1$ whereas model 3 predicts a visible difference between the decay rates of $^{14}N_2^+(v = 1)$ at different vibrational population distributions. However, our recent remeasurement of the vibrational distribution at 25 V suggests that there is a considerably less difference in the $v = 2$ to $v = 1$ population ratio between the 25 and 47 V injections than reported previously.[15] Therefore model 3 can be consistent with the experimental results. In addition, we comment on the incorrect analyses for Figures 1, 2, and 4 in ref 15 that apparently support model 4; the problem in those analyses is that the total rates of loss for $N_2^+(v = 1,2)$ are fixed constant at $0.5k_L$ and various degrees of vibrational deactivation are assumed. In a correct analysis, both the total removal rate and vibrational deactivation rate should be fitting parameters to the experimental plots, as indicated in the present work.

Discussion

The results indicate efficient deactivation of $N_2^+(v) + N_2$ and $N_2^+(v) + O_2$ that involves multiquantum vibrational transfer/loss in a single collision. The deviation from $\Delta v = -1$ deactivation is substantial. For both reactions the kinetics (and also the dynamics for $^{15}N_2^+(v) + {}^{14}N_2$) is best described by the model in which the vibration relaxes equally to each of the lower levels. This conclusion is difficult to understand within the framework of conventional models for vibrational energy transfer[10,11] but might be anticipated if the ion−molecule collisions proceed through deep attractive potential wells. It is notable that multiquantum deactivation is observed for relatively low vibrational levels ($v \leq 4$) and at low collision energy (<0.1 eV). This result is in contrast to the study of Wyttenbach and Bowers,[12] in which the deactivation of $NO^+(v)$ for $NO^+(v = 2) + CS_2$, C_2H_4, and C_3H_8 and $NO^+(v = 2, 3) + CH_3Br$ reactions proceeds exclusively via $\Delta v = -1$ processes at a similarly low collision energy. To our knowledge, the $N_2^+(v) - N_2$ and $N_2^+(v) - O_2$ reactions are rare examples of extensive $|\Delta v| > 1$ processes at thermal energy.

For neutral systems, the $|\Delta v| = 1$ rule in vibrational excitation and deactivation is a concept widely accepted for decades both experimentally and theoretically.[10,11] This rule applies quite well for neutrals in relatively low vibrational levels. According to the Landau−Teller theory for V−T energy transfer, transitions with $|\Delta v| > 1$ are forbidden when the vibrational wave functions involved can be approximated as harmonic and when the vibrational amplitude is far smaller than the "range parameter" (≈ 0.2 Å) for the repulsive part of the interaction potential. This is usually the case for lower vibrational levels in many neutral−neutral systems, and deviation from the $|\Delta v| = 1$ rule is limited, with multiquantum deactivation contributing less than 1%.[11] The theory and experiments also indicate that the V−T probability for neutral systems is small at thermal energies, typically of the order of 10^{-6} or smaller at 300 K for many systems.[10,11] When colliding neutrals have permanent dipoles or dipole derivatives, the dipole−dipole interaction can significantly enhance the vibrational transfer probability via V−V processes.[10] For example, for hydrogen halides a pronounced correlation is found between the V−V energy gap (ΔE) and the deactivation probability and, when the process is resonant ($\Delta E \approx 0$), the probability can amount to ≈ 10% of the collision rate.[29] Nevertheless, multiquantum deactivation appears to be a rare process. Even with a high probability of deactivation due to the strong HF−HF attraction (≈ 0.3 eV),[30,31] $HF(v = 4) + HF$ relaxes by single quantum processes[32,33] and the relaxation of $HF(v = 5) + HF$ is also largely (>90%) a single quantum process.[33] Deactivation with $|\Delta v| > 1$ has been observed for so-called "supercollisions", in which neutral polyatomic molecules with high vibrational excitation (20000−40000 cm^{-1}) undergo deactivation by large amounts of energy loss at ambient temperature.[34−37] In view of the above, it appears that the multiquantum deactivation for $N_2^+(v) - N_2$ and $N_2^+(v) - O_2$ can only be accounted for by the different potential energy curves that are specific to ion−molecule systems.

Compared to neutral−neutral systems, ion−molecule interactions are characterized by significantly deeper intermolecular potential wells. The large well depths may be correlated with the multiquantum vibrational deactivations observed for the collisions of $N_2^+(v \geq 2)$ with N_2 and O_2. The potential wells are exceptionally deep for $N_2^+-N_2$ and $N_2^+-O_2$. For the $N_2^+-N_2$ system, measurements report 1.12 ± 0.07 eV[38] and 1.09 ± 0.09 eV[39] for the bond energy of the N_4^+ ion−molecule complex. The large well depth arises from the stabilization due

to the resonant, electron-exchange interaction proposed by Gislason and Ferguson.[40] The well depth of the $N_2^+-O_2$ system is experimentally unknown, but we estimated the well depth to be ≈ 0.8 eV[21] by invoking a near-resonant, electron-exchange stabilization mechanism involving an electronically excited $O_2^+(a^4\Pi_u)$ state,[24]

$$N_2^+ + O_2 \rightarrow N_2 + O_2^+(a^4\Pi_u) - 0.523\ \text{eV} \qquad (15)$$

where all the species are in vibrational ground states. The stabilization in these systems is significantly greater than expected from simple electrostatic (e.g., charge-induced dipole) interactions of ≈ 0.2 eV. We believe that the multiquantum deactivations for $N_2^+(v) - N_2$ and $N_2^+(v) - O_2$ can be explained in terms of the large well depths and/or the electron-exchange interaction itself. By comparison, the NO^+-CS_2, C_2H_4, C_3H_8, and CH_3Br charge-transfer systems are off-resonant by $\sim$1 eV [I.P.(NO) = 9.26 eV while I.P.'s for CS_2, C_2H_4, C_3H_8, and CH_3Br are 10.07, 10.51, 10.95, and 10.54 eV, respectively],[41] and hence the electron-exchange interactions are expected to be significantly smaller.

The strong electron-exchange interactions and the resulting attractive forces for $N_2^+-N_2$ and O_2 would facilitate (i) an effective increase of the collision energy between N_2^+ and the neutrals, (ii) longer lifetimes for the ion−molecule complexes, and (iii) formation of charge-transfer intermediate states within the complexes. Breakdown of the $|\Delta v| = 1$ rule in the Landau−Teller theory due to high collision energies is discussed in detail by Sharp and Rapp,[42] and mechanism i could provide a feasible explanation for the multiquantum vibrational deactivations for the $N_2^+(v) + N_2$ and O_2 systems. However, it is questionable whether a maximum collision energy of ≈ 1 eV (i.e., the potential well depths for $N_2^+ + N_2$ and $N_2^+ + O_2$) could effectively open up $|\Delta v| > 1$ transitions. Exploration of this mechanism would require detailed trajectory calculations based on accurate potential energy surfaces, which are beyond the scope of the present study. In the following, we discuss the feasibility of other mechanisms ii and iii.

Ferguson[8] proposed a mechanism of vibrational predissociation of ion−molecule complexes to account for the vibrational deactivation of gaseous ions. The idea is that the ion vibrational energy flows into weak intracomplex bonds within the complex lifetime and gives rise to the complex dissociation, resulting in V−T deactivation of the ion. The deactivation rate constants for the $O_2^+(v) - M$ and $NO^+(v) - M$ systems are found to correlate with the three-body association rate constants,[8] which are proportional to the complex lifetimes. The large deactivation rate constants observed for $N_2^+(v) + N_2$ and $N_2^+(v) + O_2$ can be explained by the large bond energies and the long lifetimes for the complexes; the lifetime of N_4^+ is established to be $\sim$100 ps at thermal energy.[43] However, this mechanism might not account for the multiquantum deactivation of $N_2^+(v)$ if the energy flow into the weak intracomplex bonds is stepwise. Once the $N_2^+(v = i)$ unit dissipates the first vibrational quantum into the weak bonds, this will trigger the dissociation of the complex, and thus a successive vibrational loss from $N_2^+(v = i - 1)$ would not occur within the complex lifetime. Wyttenbach and Bowers[12] invoked this "clock" mechanism to rationalize the absence of multiquantum deactivation for $NO^+(v)$. The $v = 2 \rightarrow v = 2$ transfer in $^{15}N_2^+(v = 2) + {}^{14}N_2$ is also difficult to explain in terms of the vibrational predissociation mechanism.

To explain the observed two-quantum V−V transfer in $^{15}N_2^+(v = 2) + {}^{14}N_2$, we proposed a mechanism whereby efficient vibrational energy transfer takes place between the two high-frequency N_2 moieties in the $(^{15}N_2-{}^{14}N_2)^+$ complex and energy flow into the weak intracomplex modes is relatively inefficient.[14,15] The product state distribution given by model 4 (Table 1) indicates a V−V transfer with $|\Delta v| = 2$ only, i.e., formation of $(2^+,0)$, $(2,0^+)$, $(0^+,2)$, and $(0,2^+)$ product states, while that for model 3 indicates that the vibrational energy is somewhat randomized among these high-frequency moieties, i.e., formation of $(2^+,0)$, $(2,0^+)$, $(1^+,1)$, $(1,1^+)$, $(0^+,2)$, and $(0,2^+)$ states. In photodissociation of N_4^+ clusters followed by detection of vibrational excitation in the N_2^+ fragment,[44] Bieske proposed a model that predicts a product vibrational state distribution similar to that of model 3.

A mechanism of intracomplex V−V energy transfer between the high-frequency moieties, however, might not be able to account for the multiquantum deactivation in $N_2^+(v)-O_2$, if the V−V transfer is stepwise. This is because the N_2 and O_2 moieties in the $[N_2-O_2]^+$ collision complex have a poor energy match, given the vibrational constants for the isolated species N_2^+ ($\omega_e = 2207.37$ cm^{-1}), O_2 ($\omega_e = 1580.39$ cm^{-1}), N_2 ($\omega_e = 2358.57$ cm^{-1}), and O_2^+ ($\omega_e = 1906.07$ cm^{-1}).[28] Even with intracomplex V−V transfer between the highest-frequency N_2 and O_2 moieties, a substantial amount of excess energy would have to be dissipated into the weak bonds of the $[N_2-O_2]^+$ complex upon the first V−V transfer and the complex would dissociate before the second vibration is transferred. A possible alternative is that the strong attractive interactions might create a significant matrix element for direct, multiquantum V−V transfer.

For the collisions of $N_2^+(v = 2)$ with O_2, another consideration is the formation of an intermediate charge-transfer complex $[N_2(v = 0)-O_2^+(a^4\Pi_u)]$, which can redissociate to yield $N_2^+(v < 2) + O_2(X,v)$ via the reverse CT transitions. The existence of the CT complex is strongly suggested by the favorable energetics (exothermic by 0.012 eV at infinite separation, eq 3), strong coupling of the states (the very fast reverse reaction, $O_2^+(a^4\Pi_u) + N_2 \rightarrow O_2 + N_2^+$),[45] and the observed CT enhancement for $N_2^+(v \geq 2) + O_2$, which is probably due to the production of $O_2^+(a^4\Pi_u)$. The Franck−Condon overlaps for the reverse CT transitions would favor the formation of $N_2^+(v = 0)$ ($\Delta v = -2$ deactivation) rather than of $N_2^+(v = 1)$ ($\Delta v = -1$ deactivation), i.e., 0.917 and 0.078 for $N_2(v = 0) \rightarrow N_2^+(v = 0)$ and $N_2(v = 0) \rightarrow N_2^+(v = 1)$ transitions, respectively. Corresponding Franck−Condon factors for the $O_2^+(a^4\Pi_u, v = 0) \rightarrow O_2(X, v)$ transitions also favor the $\Delta v = -2$ channel for $N_2^+(v = 2)$; calculated Franck−Condon factors for $O_2^+(a^4\Pi_u, v = 0)-O_2(X, v)$ transitions for the most energy-resonant product channels, $N_2^+(v = 0) + O_2(v = 3)$ and $N_2^+(v = 1) + O_2(v = 1)$, are 0.214 and 0.054, respectively.[46]

The existence of intermediate charge-transfer states for the $N_2^+ + N_2$ collisions is strongly suggested by the efficient charge equilibration ($k = 0.5k_L$) observed for $^{15}N_2^+(v = 0) + {}^{14}N_2$.[15] For the $[^{15}N_2-{}^{14}N_2]^+$ system originating from $^{15}N_2^+(v = 2) + {}^{14}N_2$, all the charge-transfer transitions for the network of $(2^+,0)$, $(2,0^+)$, $(1^+,1)$, $(1,1^+)$, $(0^+,2)$, and $(0,2^+)$ states have good energy resonance within ± 0.039 eV. Sequences of charge-transfer transitions, e.g., $(2^+,0) \rightarrow (1,1^+) \rightarrow (0^+,2)$, can result in two-quantum vibrational deactivation of $^{15}N_2^+(v = 2)$. We examined the evolution of product vibrational states through multiple transitions within the charge-transfer reaction network, using the CT probabilities for each step which are derived in a manner similar to those for $N_2^+(v) + Kr$ (ref 4) and $N_2^+(v) + Ar$ (ref 49) charge-transfer reactions. The calculation shows that, as the number of CT transitions increases, the initial state $(2^+,0)$ is rapidly depleted while other states develop toward a product distribution similar to that of model 3 (Table 1).

Despite the qualitative approaches above, the contribution of intermediate charge-transfer states should not be ignored even when considering other mechanisms of multiquantum vibrational deactivation, since the large well depths for $N_2^+(v) - N_2$ and $N_2^+(v) - O_2$ arise from the electron-exchange interactions in any event. The absence of multiquantum deactivation for the $NO^+(v) + M$ (M = CS_2, C_2H_4, C_3H_8, CH_3Br) reactions[12] is consistent with the present model incorporating intermediate charge-transfer states. The charge-transfer states $NO + M^+$ are higher lying than $NO^+ + M$ at infinite separation. The polarizabilities of M are significantly greater than that of NO[41] and hence the $NO + M^+$ states would be less stabilized than $NO^+ + M$ at short distances. Thus the existence of intermediate charge-transfer states is less likely for the $NO^+(v) - M$ systems. Deactivation of $N_2^+(v)$ by NO may also proceed via multiquantum vibrational energy transfer since this system is another example with strong electron-exchange interactions.[24] Unfortunately, for this system the charge transfer (eq 1) is too fast for the vibrational deactivation (eq 2) to be analyzed in sufficient detail.[27]

Conclusion

We determined the state-specific rate constants for charge transfer and vibrational deactivation for reactions of $N_2^+(v = 0-4) + N_2$ and O_2 at thermal energies. The $N_2^+(v = 0) + N_2$ reaction proceeds at $0.5k_L$ whereas the $N_2^+(v = 1-4) + N_2$ reactions are faster at $\sim 0.7k_L$. A significant amount of vibration, in addition to charge, is transferred in the $N_2^+(v > 0) + N_2$ collision. The total rate constants for the $N_2^+(v) + O_2$ reactions are dramatically enhanced upon additional vibrational excitation. The enhancement is primarily due to increased vibrational deactivation, yet a moderate enhancement of charge transfer ($\approx 50\%$) occurs for $v \geq 2$. With the refined analysis, the total rate constants and vibrational deactivation rate constants for $N_2^+(v = 1, 2) + O_2$ are somewhat larger ($\sim 30\%$) than those previously reported.

Substantial deviation from the $\Delta v = -1$ rule is observed for the vibrational deactivations of $N_2^+(v \geq 2)$ with N_2 and O_2. For both systems, the vibrational deactivation is best described by a model in which $N_2^+(v)$ relaxes equally to each of the lower vibrational states. Our previous observation of two-quantum V−V transfer is confirmed for the $N_2^+(v = 2) + N_2$ system, although single-quantum V−V transfer and V−R, T deactivation are also found to be competing processes. The observed multiquantum deactivation of $N_2^+(v)$ is rationalized by the significantly deep potential wells for $N_2^+-N_2$ and $N_2^+-O_2$ due to near-resonant, electron-exchange interactions. Multiquantum vibrational transfer can occur within the long-lived ion−molecule complexes or can also occur via multiple charge-transfer transitions during a single collision, which result in net vibrational transfer.

Acknowledgment. The authors gratefully acknowledge the financial support of the U.S. Air Force Office of Scientific Research. The AFOSR support for hypersonics research is greatly appreciated. S.K. also thanks Dr. Akitomo Tachibana for his stimulating discussions.

References and Notes

(1) Levine, R. D.; Bernstein, R. B. *Molecular Reaction Dynamics and Chemical Reactivity*; Oxford University Press: New York, 1987.
(2) *State-Selected and State-to-State Ion-Molecular Reaction Dynamics. Part 1: Experiment. Part 2: Theory, in Advances in Chemical Physics Series*; Ng, C.-Y., Baer, M., Eds.; John Wiley & Sons: New York, 1992; Vol. 82.
(3) Viggiano, A. A.; Morris, R. A. *J. Phys. Chem.* **1996**, *100*, 19227.
(4) Kato, S.; de Gouw, J. A.; Lin, C. D.; Bierbaum, V. M.; Leone, S. R. *J. Chem. Phys.* **1996**, *105*, 5455.
(5) Ferguson, E. E.; Fehsenfeld, F. C.; Albritton, D. L. Ion Chemistry of the Earth's Atmosphere. In *Gas-Phase Ion Chemistry*; Bowers, M. T., Ed.; Academic Press: New York, 1979; Vol. 1, pp 45−82.
(6) Abdou, W. A.; Torr, D. G.; Richards, P. G.; Torr, M. R. *J. Geophys. Res.* **1984**, *89*, 9069.
(7) (a) Coustenix, J.; Arnal, D.; Aupoix, B.; Brazier, J. Ph.; Lafon, A. *Aerospace Sci.* **1994**, *30*, 95. (b) *Workshop on the Use of Weakly Ionized Gases on Aerospace Applications*; Colorado Springs, CO, 1997.
(8) Ferguson, E. E. *J. Phys. Chem.* **1986**, *90*, 731.
(9) Ferguson, E. *Comments At. Mol. Phys.* **1990**, *24*, 327.
(10) Yardley, J. T. *Introduction to Molecular Energy Transfer*; Academic Press: New York, 1980.
(11) Kuratani, K.; Tsuchiya, S. *Shock Waves in Chemistry and Physics*; Shokabo: Tokyo, 1968.
(12) Wyttenbach, T.; Bowers, M. T. *J. Phys. Chem.* **1993**, *97*, 9573.
(13) Kato, S.; Frost, M. J.; Bierbaum, V. M.; Leone, S. R. *Rev. Sci. Instrum.* **1993**, *64*, 2808.
(14) Frost, M. J.; Kato, S.; Bierbaum, V. M.; Leone, S. R. *J. Chem. Phys.* **1993**, *98*, 5993.
(15) Frost, M. J.; Kato, S.; Bierbaum, V. M.; Leone, S. R. *J. Chem. Phys.* **1994**, *100*, 6359.
(16) McCann, K. J.; Flannery, M. R.; Hornstein, J. V.; Moran, T. F. *J. Chem. Phys.* **1975**, *63*, 4998.
(17) McAfee, K. B., Jr.; Szmanda, C. R.; Hozack, R. S.; Johnson, R. E. *J. Chem. Phys.* **1982**, *77*, 2399.
(18) Howard, S. L. *Can. J. Chem.* **1991**, *69*, 584.
(19) Sohlberg, K.; Futrell, J.; Szalewicz, K. *J. Chem. Phys.* **1991**, *94*, 6500.
(20) Sohlberg, K.; Szalewicz, K. *Chem. Phys.* **1996**, *206*, 87.
(21) Kato, S.; Frost, M. J.; Bierbaum, V. M.; Leone, S. R. *Can. J. Chem.* **1994**, *72*, 625.
(22) Dobler, W.; Howorka, F.; Lindinger, W. *Plasma Chem. Plasma Process.* **1982**, *2*, 353.
(23) Dobler, W.; Villinger, H.; Howorka, F.; Lindinger, W. *Int. J. Mass Spectrom. Ion Phys.* **1983**, *47*, 171.
(24) Ferguson, E. E.; Richter, R.; Lindinger, W. *J. Chem. Phys.* **1988**, *89*, 1445.
(25) Smith, D.; Adams, N. G. *Phys. Rev. A* **1981**, *23*, 2327.
(26) de Gouw, J. A.; Ding, L. N.; Frost, M. J.; Kato, S.; Bierbaum, V. M.; Leone, S. R. *Chem. Phys. Lett.* **1995**, *240*, 362.
(27) Frost, M. J.; Kato, S.; Bierbaum, V. M.; Leone, S. R. *Chem. Phys.* **1998**, *231*, 145.
(28) Laher, R. R.; Gilmore, F. R. *J. Phys. Chem. Ref. Data* **1991**, *20*, 685.
(29) Horwitz, A. B.; Leone, S. R. *J. Chem. Phys.* **1978**, *69*, 5319.
(30) Smith, D. F. *J. Mol. Spectrosc.* **1959**, *3*, 473.
(31) Poulsen, L. L.; Billing, G. D.; Steinfeld, J. I. *J. Chem. Phys.* **1978**, *68*, 5121.
(32) Douglas, D. J.; Moore, C. B. *Chem. Phys. Lett.* **1978**, *57*, 485.
(33) Jursich, G. M.; Crim, F. F. *J. Chem. Phys.* **1981**, *74*, 4455.
(34) Hassoon, S.; Oref, I.; Steel, C. *J. Chem. Phys.* **1988**, *89*, 1743.
(35) Toselli, B. M.; Barker, J. R. *J. Chem. Phys.* **1991**, *95*, 8108.
(36) Hartland, G. V.; Qin, D.; Dai, H.-L. *J. Chem. Phys.* **1994**, *101*, 8554.
(37) Mullin, A. S.; Michaels, C. A.; Flynn, G. W. *J. Chem. Phys.* **1995**, *102*, 6032.
(38) Hiraoka, K.; Nakajima, G. *J. Chem. Phys.* **1988**, *88*, 7709.
(39) Norwood, K.; Luo, G.; Ng, C. Y. *J. Chem. Phys.* **1989**, *91*, 849.
(40) Gislason, E. A.; Ferguson, E. E. *J. Chem. Phys.* **1987**, *87*, 6474.
(41) *CRC Handbook of Chemistry and Physics*, 75 ed.; Lide, D. R., Ed.; CRC Press: Boca Raton, FL, 1994.
(42) Sharp, T. E.; Rapp, D. *J. Chem. Phys.* **1965**, *43*, 1233.
(43) van Koppen, P. A. M.; Jarrold, M. F.; Bowers, M. T.; Bass, L. M.; Jennings, K. R. *J. Chem. Phys.* **1984**, *81*, 288.
(44) Bieske, E. *J. Chem. Phys.* **1993**, *98*, 8537.
(45) Lindinger, W.; Albritton, D. L.; McFarland, M.; Fehsenfeld, F. C.; Schmeltekopf, A. L.; Ferguson, E. E. *J. Chem. Phys.* **1975**, *62*, 4101.
(46) The Franck−Condon factors are calculated using spectroscopic parameters in refs 28 and 47 and the procedure by Nicholls (ref 48).
(47) Herzberg, G. *Molecular Spectra and Molecular Structure. I. Spectra of Diatomic Molecules*; Van Nostrand Reinhold: New York, 1950.
(48) Nicholls, R. W. *J. Res. Natl. Bur. Stand. A* **1961**, *65A*, 451.
(49) Kato, S.; de Gouw, J. A.; Lin, C. D.; Bierbaum, V. M.; Leone, S. R. *Chem. Phys. Lett.* **1996**, *256*, 305.